Supporting Information

Molybdenum Trioxide Nanoparticles with Intrinsic Sulfite Oxidase Activity

*Ruben Ragg,[†] Filipe Natalio,[‡] Muhammad Nawaz Tahir,[†] Henning Janssen,[§] Anubha Kashyap,[§] Dennis Strand,[§] Susanne Strand,[§] Wolfgang Tremel [†,]**

[†]Institut für Anorganische Chemie und Analytische Chemie, Johannes-Gutenberg-Universität, Duesbergweg 10–14, D-55099 Mainz, Germany, [‡]Institut für Chemie - Anorganische Chemie, Martin-Luther Universität Halle-Wittenberg, Kurt Mothes Straße 2, D-06120 Halle, Germany, [§]Medizinische Klinik, Johannes-Gutenberg-Universität, Obere Zahlbacher Strasse 63, D-55131 Mainz, Germany, *email: tremel@uni-mainz.de

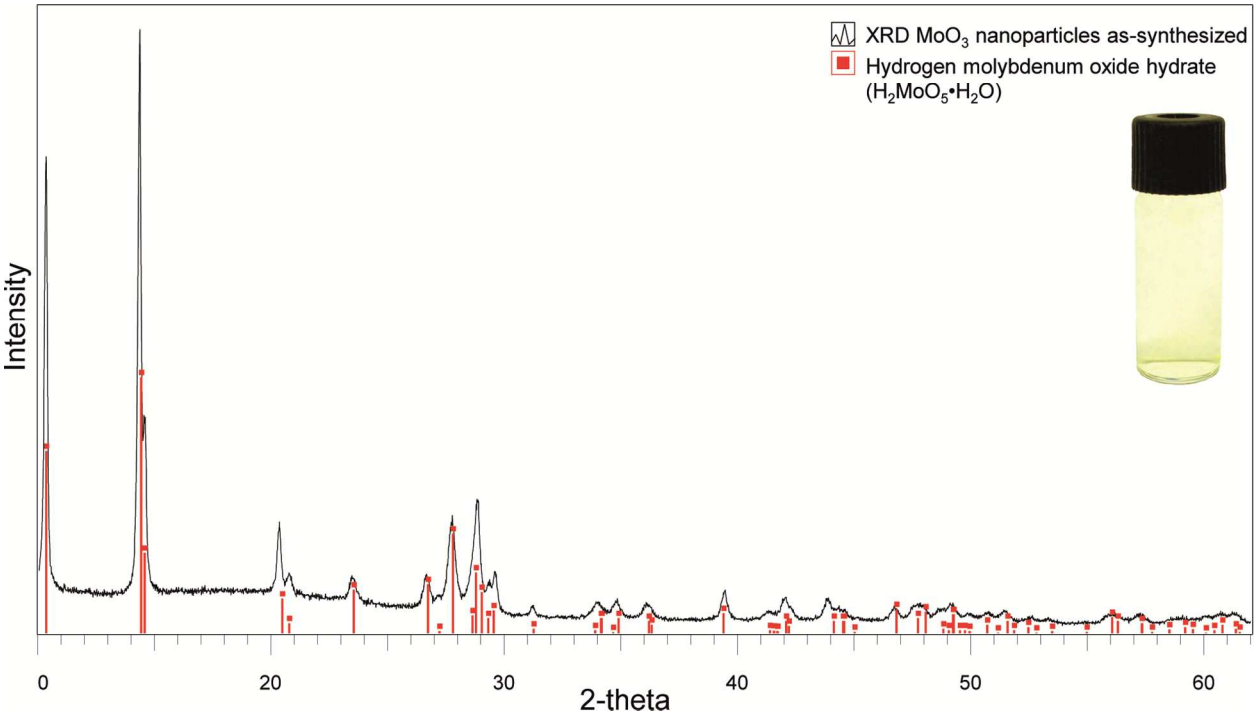

Figure S1. P-XRD pattern of as-synthesized MoO_3 nanoparticles and digital photograph of respective nanoparticle dispersion [0.5 mg/ml]. P-XRD showed the formation of the hydrated form of monoclinic hydrogen molybdenum oxide ($H_2MoO_5•H_2O$). The nanoparticles displayed a solubility of up to 1 mg/ml in distilled water.

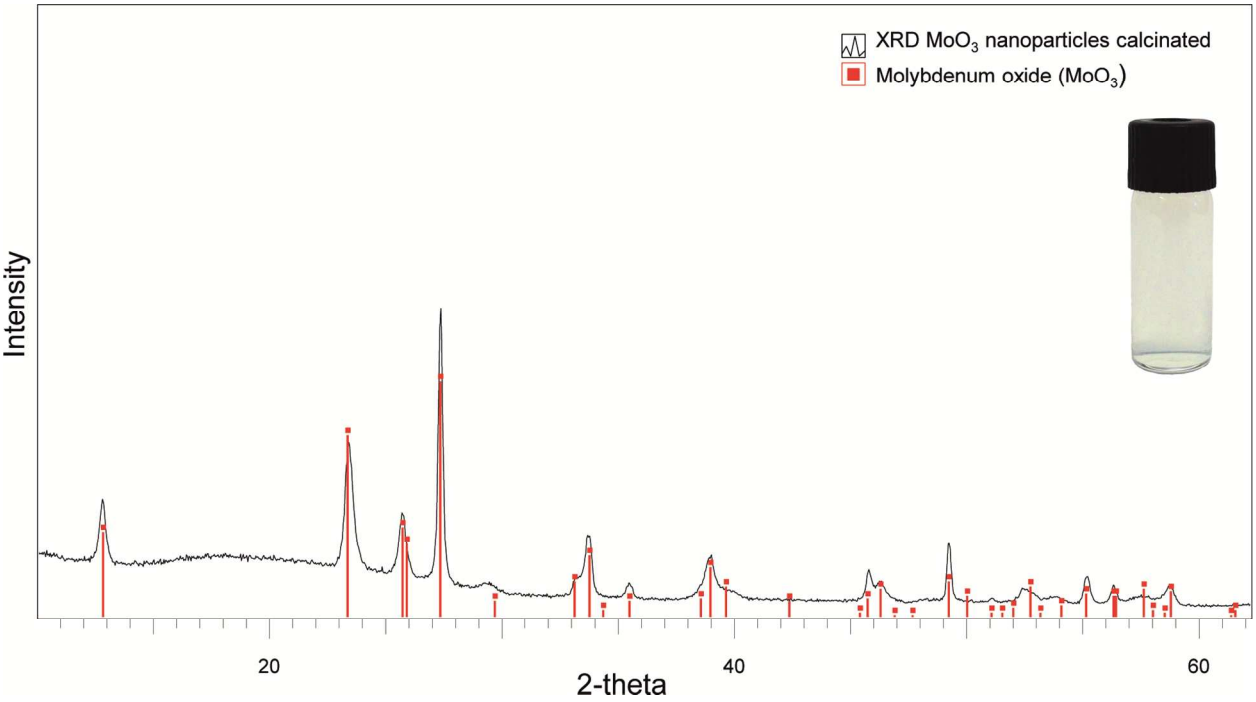

Figure S2. P-XRD pattern of calcinated MoO_3 nanoparticles and digital photograph of respective nanoparticle dispersion [0.5 mg/ml]. P-XRD shows the formation of phase pure orthorhombic molybdenum oxide (MoO_3). The nanoparticles remained well soluble up to 1 mg/ml in distilled water after calcination.

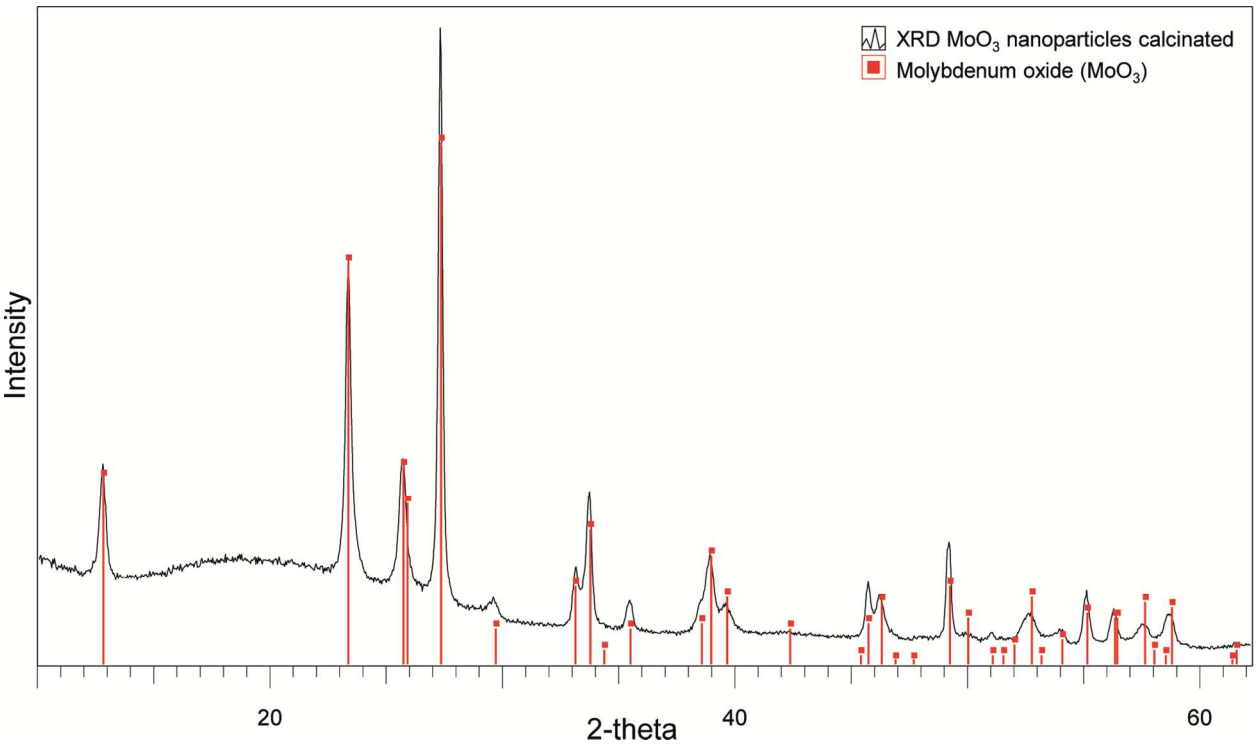

Figure S3. P-XRD pattern of calcinated MoO_3 nanoparticles after incubation in bovine serum. MoO_3 nanoparticles were incubated in bovine serum for six hours. After separation from the serum the particles were examined by P-XRD, still showing phase-pure orthorhombic molybdenum oxide (MoO_3).

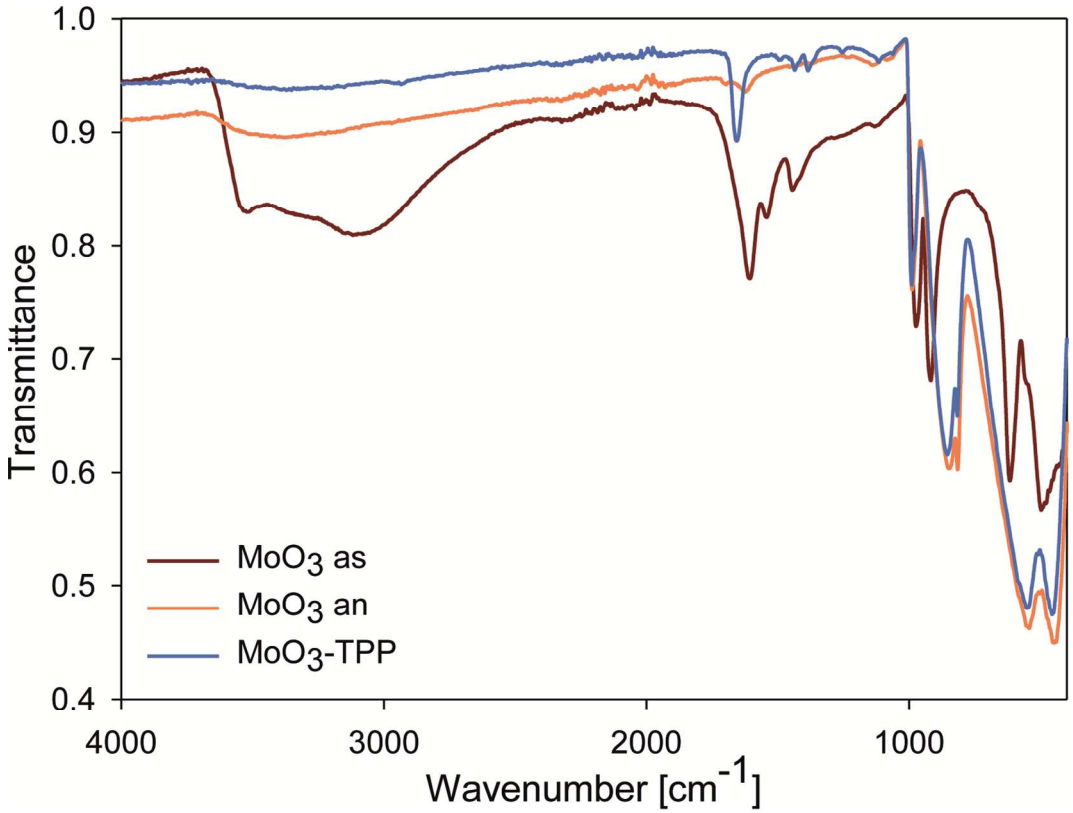

Figure S4. IR-Measurements of as-synthesized (MoO_3 as), calcinated (MoO_3 an) and TPP-functionalized (MoO_3-TPP) MoO_3 nanoparticles. The bands corresponding to the O-H stretch (from H_2O) at 3520-3100 cm^{-1} and 1610 cm^{-1} are clearly observed for as-synthesized MoO_3 nanoparticles corroborating the idea of the presence of a high degree of hydration either between layers or at the surface of the nanoparticles in agreement with P-XRD data. After calcination, a clear reduction of the intensity of these bands indicates the elimination of H_2O. The typical bands for the Mo=O terminal bond at 990 cm^{-1} and Mo-O-Mo bridging bonds at 860 cm^{-1} confirm the orthorhombic symmetry of the calcinated MoO_3 nanoparticles. The bands found at 550 and 455 cm^{-1} are attributed to the terminal Mo-O stretch. The band at 920 cm^{-1} corresponding to the vibration of O atoms in peroxo groups (O-O) of as-synthesized nanoparticles, disappears after temperature treatment (450ºC, 30 min). The band at 1660 cm^{-1} corresponds to primary amide groups (C=O and C-N) from Dopa-TPP and shows the successful surface functionalization.

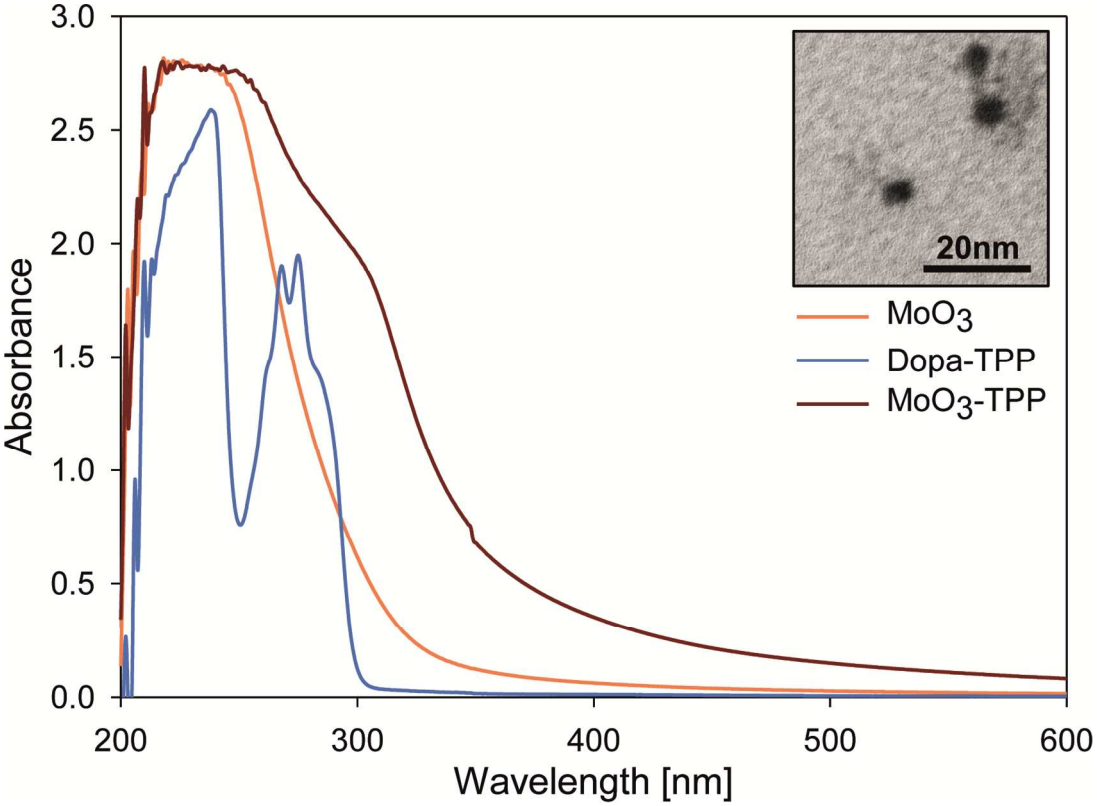

Figure S5. UV-VIS-Spectra of Dopa-TPP ligand, MoO_3 and MoO_3-TPP nanoparticles and TEM-image of MoO_3-TPP nanoparticles. Calcinated MoO_3 nanoparticles exhibit no prominent absorption characteristics, with one band having a maximum at 230 nm attributed to Mo-O ligand to metal charge transfer (LMCT). The spectrum of the Dopa-TPP ligand exhibits a broad band at 270 nm, which can also be found as a shoulder in the LMCT peak of the MoO_3-TPP spectrum and therefore proves the successful surface functionalization of the particles. The inset shows a transmission electron microscopy image of the functionalized MoO_3-TPP nanoparticles.

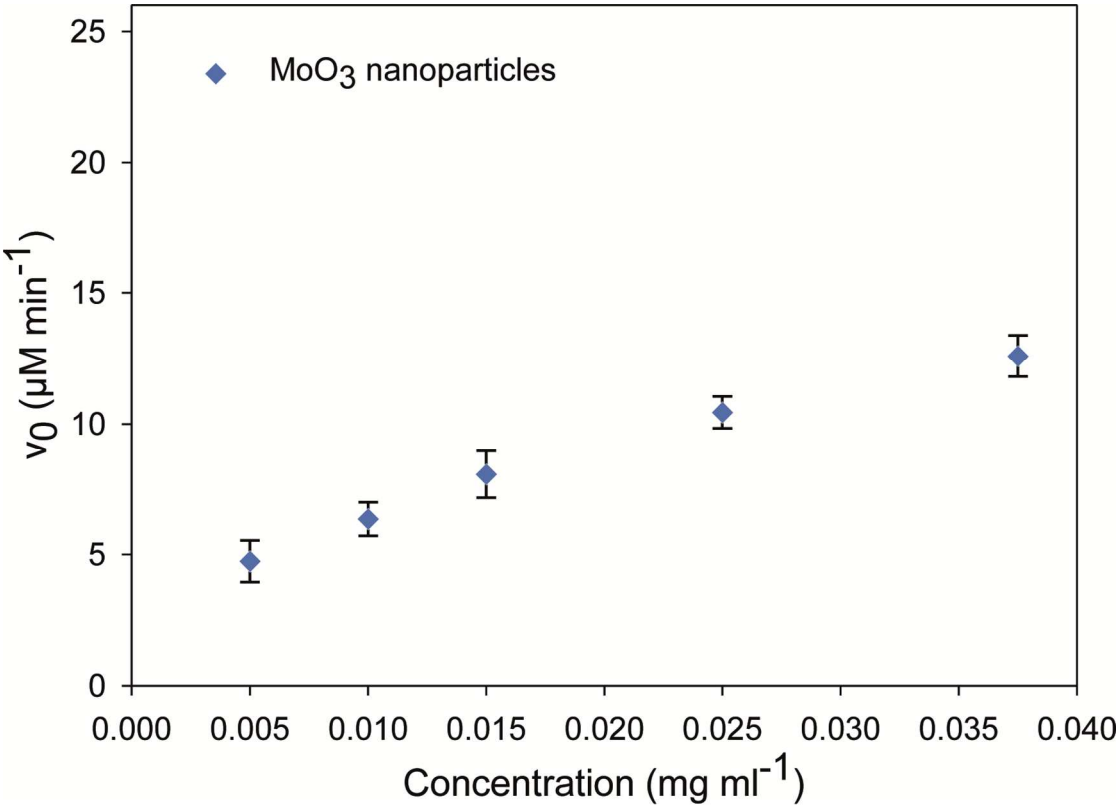

Figure S6. Concentration dependence of the sulfite oxidase activity of MoO_3 nanoparticles. Concentration dependence of the sulfite oxidase activity of calcinated MoO_3 nanoparticles, determined by measuring the initial reaction rates of the ferricyanide reduction from the absorption at 420 nm for 180 s at 25 ºC in the presence of constant concentrations of SO_3^{2-} (0.66 mM) and potassium ferricyanide (0.33 mM).

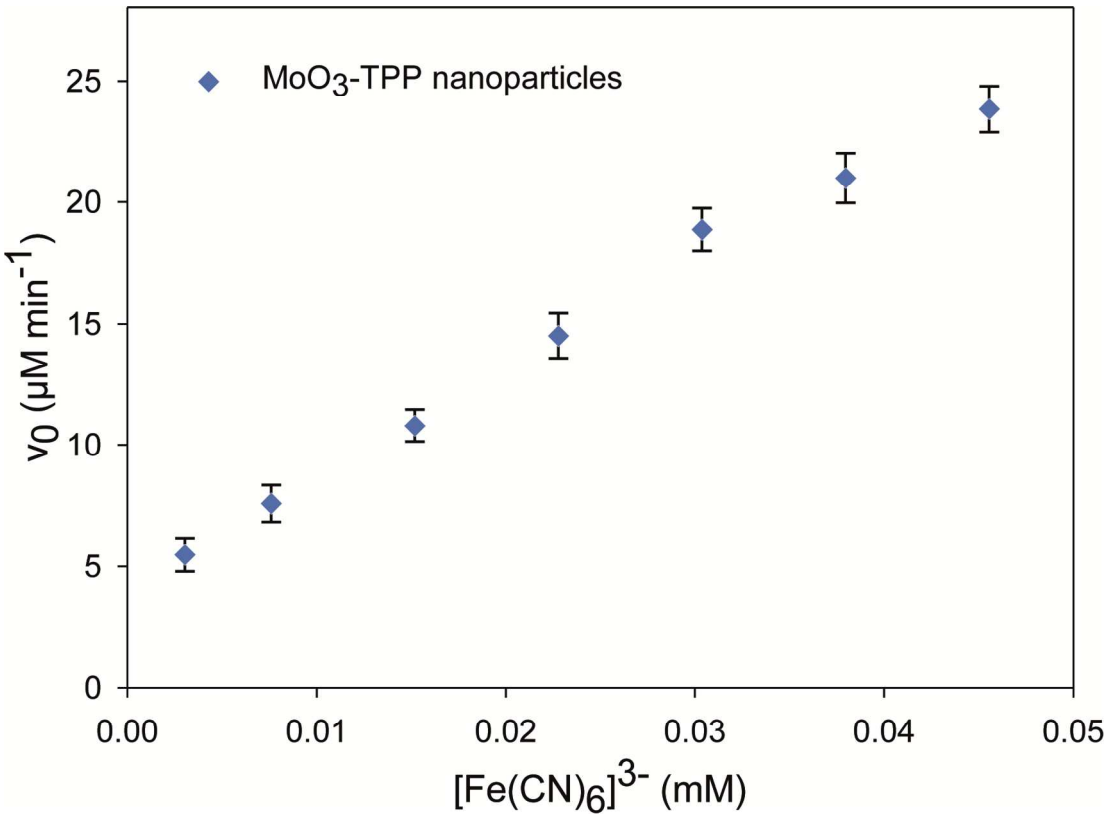

Figure S7. Dependence of the sulfite oxidase activity of TPP-functionalized MoO_3 nanoparticles on the ferricyanide concentration. Dependence of the sulfite oxidase activity of functionalized MoO_3-TPP nanoparticles on the ferricyanide concentration, determined by measuring the initial reaction rates of the ferricyanide reduction from the absorption at 420 nm for 180 s at 25 ºC in the presence of constant concentrations of SO_3^{2-} (0.66 mM) and MoO_3-TPP nanoparticles (0.025 mg/ml).

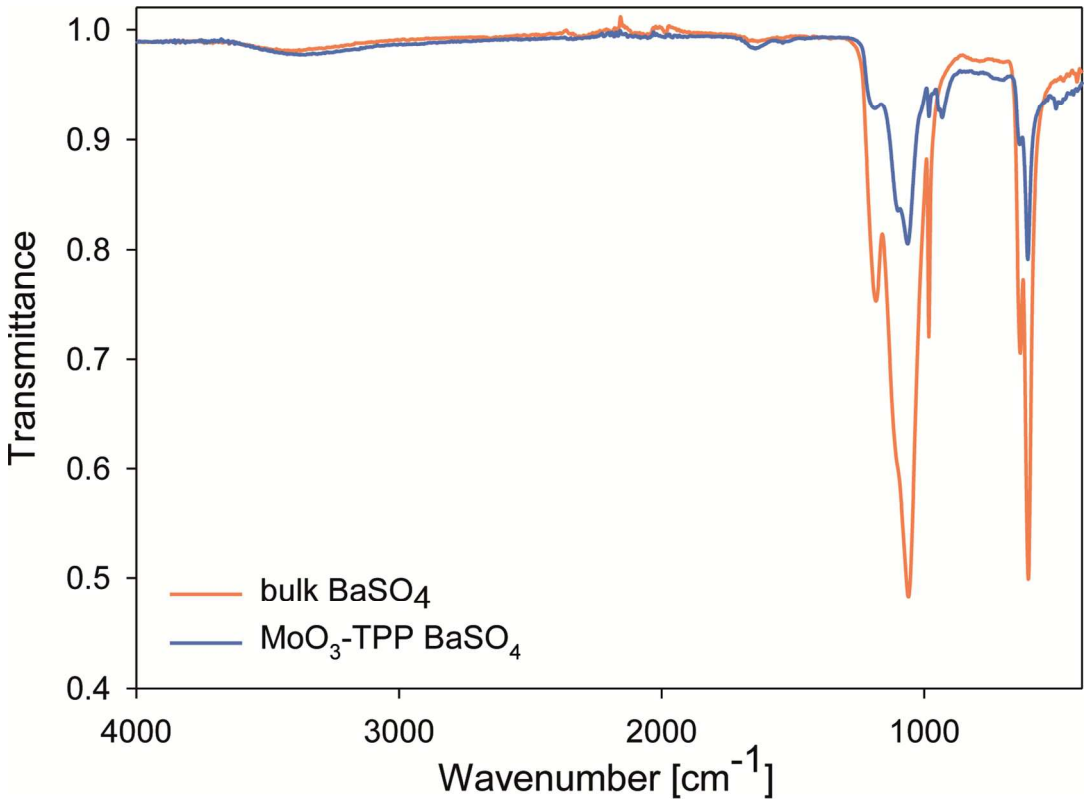

Figure S8. IR-Spectra of $BaSO_4$ formed by the reaction of sulfite with MoO_3-TPP and bulk $BaSO_4$. The bands corresponding to bulk $BaSO_4$ at 1061 cm^{-1} (S-O stretch) and 605 cm^{-1} are clearly observed in the precipitate formed (addition of 8.5 mM barium chloride to reaction mix) after the reaction of sulfite with MoO_3-TPP nanoparticles (1 h, RT) and therefore demonstrates the MoO_3-TPP mediated formation of sulfate.

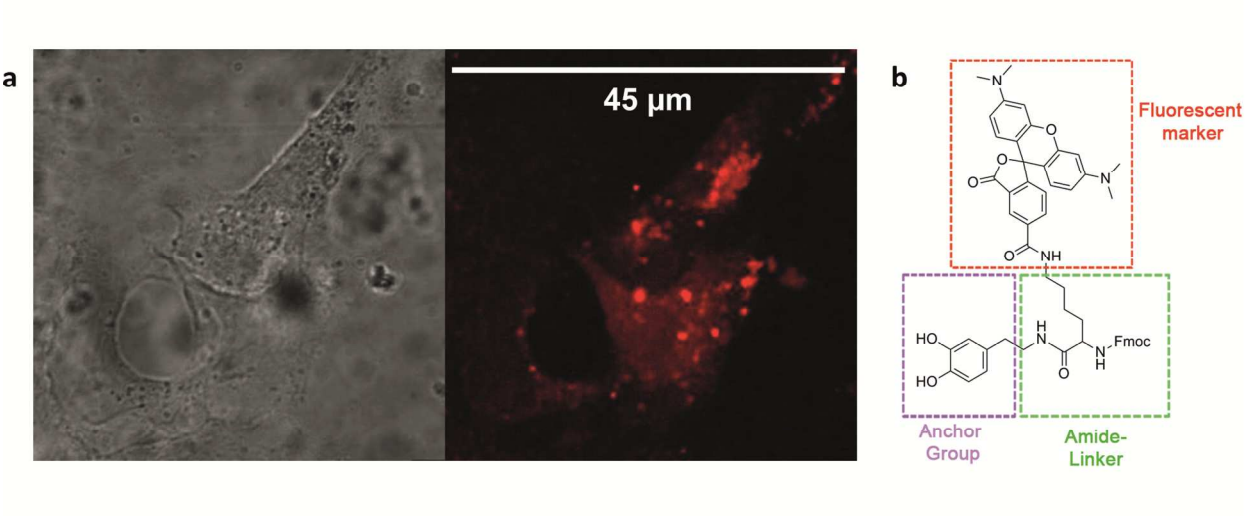

Figure S9. Cell-uptake studies with Fmoc-TAMRA functionalized MoO_3 nanoparticles. LSM localization studies in HepG2 cells with TAMRA-labeled MoO_3-TAMRA nanoparticles (50 ppm, 8 h, λ_{ex}=543 nm) showing cellular uptake of the particles but no intracellular localization at the mitochondria.

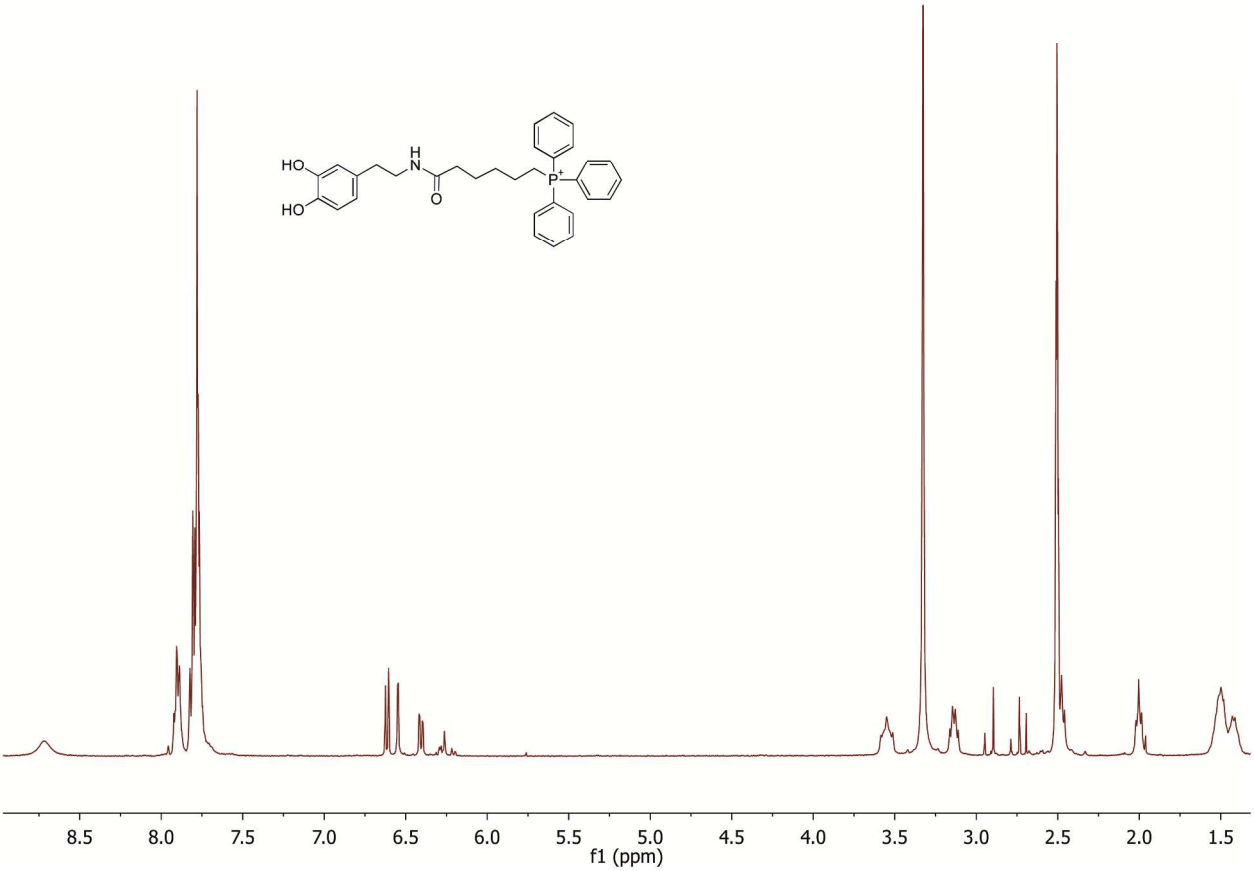

Figure S10. ^{1}H-NMR of Dopamine-TPP (1).

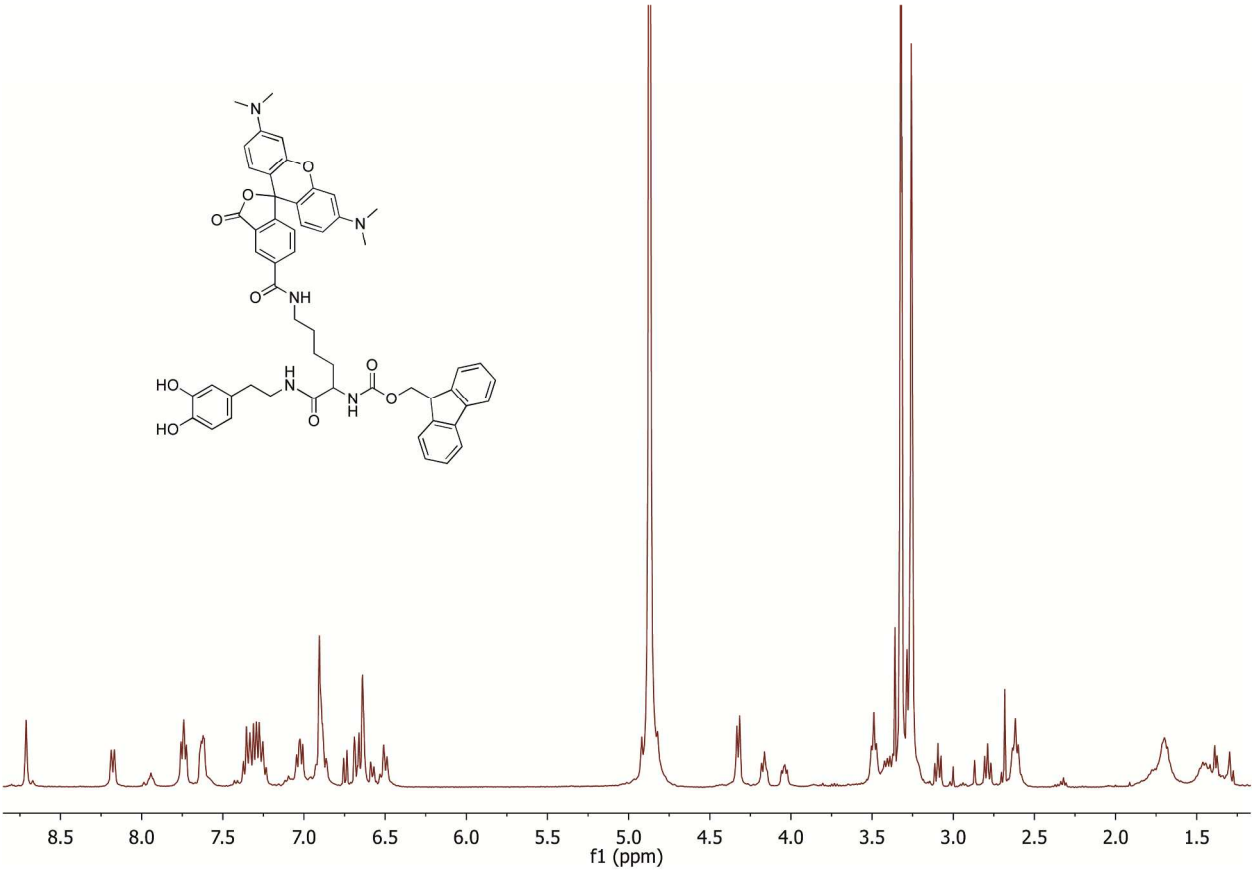

Figure S11. ^{1}H-NMR of Dopamine-Lys(5-TAMRA)-Fmoc (2).

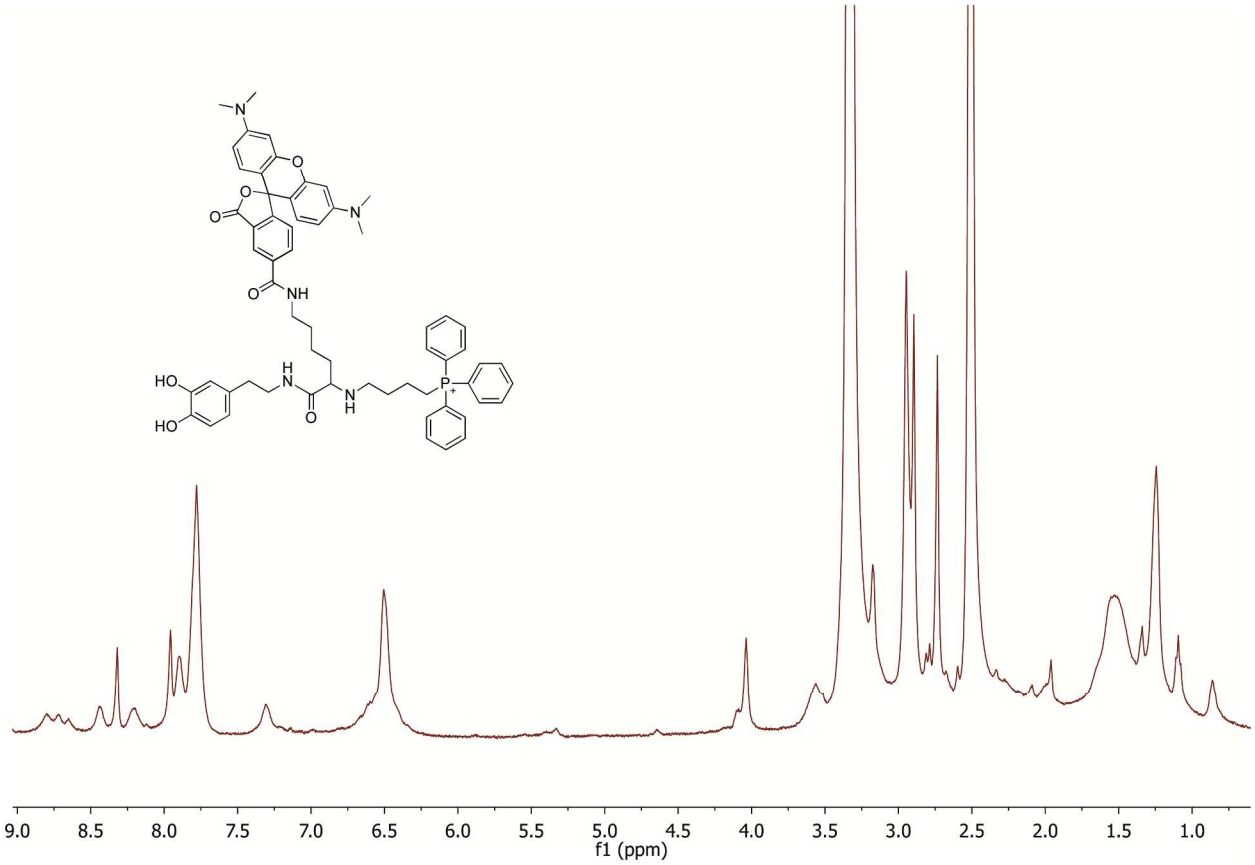

Figure S12. ^{1}H-NMR of Dopamine-Lys(5-TAMRA)-TPP.